pH effect on the assembly of metal–organic architectures

La-Sheng Long*

Crystal engineering is the rational design and assembly of solid-state structures with desired properties *via* the manipulation of intermolecular interactions, hydrogen bonding and metal–ligand complexation in particular. The heart of crystal engineering is to control the ordering of the building blocks, be they molecular or ionic, toward a specific disposition in the solid state. The relatively weak strength of intermolecular forces with respect to chemical bonding renders the assembly of supramolecular constructs sensitive to external physical and chemical stimuli, with pH condition of the reaction mixture being arguably the most prominent and extensively observed. Using selected examples of constructing metal–organic architectures from recent literature, the influences of pH on the specific ligand forms, the generation and metal coordination of hydroxo ligands, ligand transformation promoted by pH condition changes, pH-dependent kinetics of crystallization of a number of metal–organic architectures are discussed. Current status of this particular areas of research in supramolecular chemistry and materials are assessed and personal perspectives as to toward what directions should this chemistry head are elaborated.

1 Introduction

Crystal engineering, which was first used in 1955,[1] is "the understanding of intermolecular interactions in the context of crystal packing and the utilization of such understanding in the design of new solids with desired physical and chemical properties".[2] Its essence is the manipulation of intermolecular interactions by which molecular ordering of building blocks in the solid state may be controlled and materials with desired properties may be produced.[3] Among the different types of intermolecular forces, such as $\pi\cdots\pi$,[4] halogen$\cdots$halogen,[5] Au$\cdots$Au[6] and ionic interactions,[7] all have been exploited in crystal engineering studies so far, hydrogen bonding and metal–ligand complexation are most extensively studied in crystal engineering as they are directional and significantly stronger than the other intermolecular interactions.[8] These forces are nevertheless rather weak, and ensembles due to the collective stabilization of such forces are still susceptible to external physical or chemical perturbations such as solvent participation in crystallization or temperature change to the same reaction mixture.[9,10]

The pH condition of a reaction mixture represents another important factor with which one may control the outcome of crystal engineering, in particular in the construction of metal–organic architectures.[11] The pH influences are due to (1) the specific ligand forms are frequently dependent on the degree of the ligand protonation; (2) the generation of hydroxo ligand is strongly dependent on the pH condition of the reaction if it is carried out in aqueous solutions; (3) the coordination of ancillary ligands are also dependent on the pH condition; (4) *in situ* formation of ligands that are different from the original ones may be possible depending on the reaction pH conditions; and (5) the reaction kinetics can be controlled by altering pH conditions. The specific forms of ligands, potentially coordinating OH groups and ligands produced *in situ* all contribute to the complexity of metal–ligand complexation as well as the packing of the building blocks upon crystallization, while reaction kinetics control through pH change may lead to crystallization of bulk solid state materials with unusual properties such as optical activity. Using selected examples from recent literature, this

State Key Laboratory of Physical Chemistry of Solid Surface and Department of Chemistry, College of Chemistry and Chemical Engineering, Xiamen University, Xiamen, 361005. E-mail: lslong@xmu.edu.cn; Fax: + 86-592-218-3047

La-Sheng Long received his B.S. and M.S. degrees in chemistry respectively from Anhui Normal University in 1986 and Lanzhou University in 1989, and his Ph.D. from Zhongshan University in 1999. He is now a professor of Xiamen University. His current research is focused on the synthetic and materials chemistry of cluster compounds of lanthanide-transition metal elements.

La-Sheng Long

Highlight aims to illustrate the profound influences of pH conditions on the construction of metal–organic architectures. Specifically, the discussion will be focusing on the construction of metal–organic architectures featuring carboxylates, polyoxometalates, and imidazole derivatives as key framework-building ligands. Wherever appropriate, the participation of ancillary ligands, in particular those based on dipyridyl moieties and small-unit ligand derived from water are noted.

2 pH effect on the topology of metal–organic architectures

2.1 pH effect on the structure of carboxylate-based metal–organic architectures

Carboxylate ligands represent an important class of functional building units in the assembly of supramolecular architectures.[12] Numerous structurally diverse metal–organic frameworks have been constructed mainly due to the versatile coordination modes (Chart 1)[12e] of carboxylato ligands whose specific forms are highly dependent on the pH condition of the reaction mixture. As these different forms coordinate to a particular metal ion in drastically different fashion, the resulting metal–organic architectures are sensitively dependent on the pH conditions. In addition, the carboxylato group is frequently involved in hydrogen bonding interactions, both as hydrogen-bond donors (when it is protonated) and acceptors; hydrogen bonding plays an important role in determining the solid state arrangement of the building blocks.[12]

For this particular class of supramolecular assemblies, the most frequently observed effects caused by changing pH conditions is the different dimension of the resulting metal–organic architectures.[11,13–24] For example, the reaction of cupric acetate with benzoic acid and 4,4′-bpy in methanol–water solution at pH = 5.5 produced the mononuclear [Cu(H$_2$O)(benzoate)$_2$(4,4′-bpy)$_2$](benzoic acid)$_2$·(4,4′-bpy) (1) (Fig. 1),[14] while at pH = 6.0, two dimeric copper(II) complexes, [Cu$_2$(H$_2$O)$_2$(benzoate)$_4$(4,4′-bpy)$_3$]·(H$_2$O)$_9$ (2) (Fig. 2) and [Cu$_2$(benzoate)$_4$(4,4′-bpy)$_3$] (3) (Fig. 3), were obtained. Using the same reaction mixture, the one-dimensional (1D) coordination polymer of [Cu$_3$(H$_2$O)$_4$(benzoate)$_6$(4,4′-bpy)$_{4.5}$]·(4,4′-bpy)·(H$_2$O)$_5$ (4) (Fig. 4) resulted at pH = 7.5. Upon further increasing pH to 8.0 afforded the 2D structure of [Cu$_3$(OH)$_2$(H$_2$O)$_2$(benzoate)$_4$(4,4′-bpy)$_2$] (5) (Fig. 5). On the basis of the components of 1 to 5, it is clear that the pH effect on the structures of 1 to 5 is in fact on the
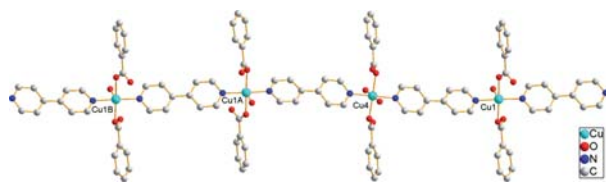

Chart 1
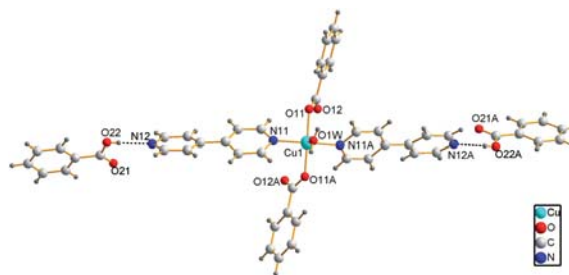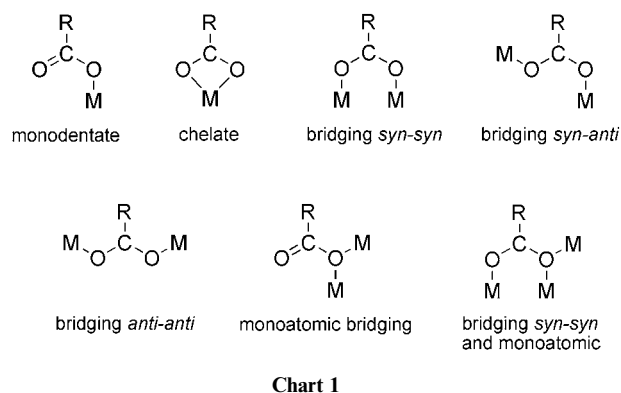
Fig. 1 ORTEP plot showing the structure of **1**. (Reprinted with permission from ref. 14. Copyright 2007 The American Chemical Society.)
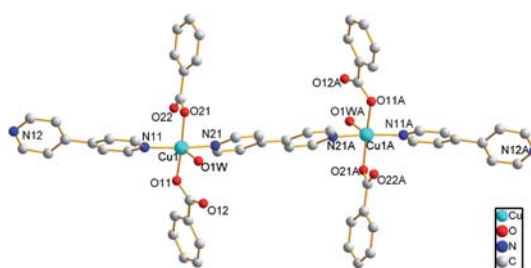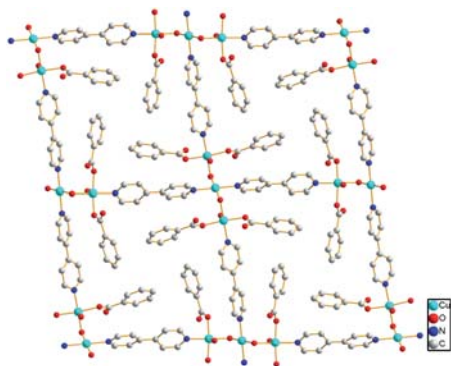

Fig. 2 ORTEP plot showing the structure of the copper(II) dimer in **2**. (Reprinted with permission from ref. 14. Copyright 2007 The American Chemical Society.)
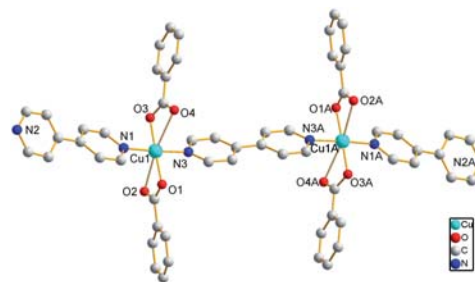
Fig. 3 ORTEP plot showing the structure of the copper(II) dimer in **3**. (Reprinted with permission from ref. 14. Copyright 2007 The American Chemical Society.)

Fig. 4 ORTEP plot showing the 1D chain in **5**. (Reprinted with permission from ref. 14. Copyright 2007 The American Chemical Society.)
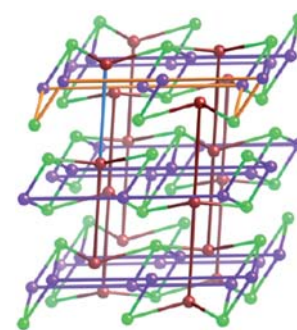

Fig. 5 ORTEP plot showing the 2D structure of **5** viewed along the *a*-axis. (Reprinted with permission from ref. 14. Copyright 2007 The American Chemical Society.)

Fig. 7 Schematic view of the overall trinodal 4-connected 3D net in **7**. The layers in the previous figure are connected by interlayer bpa bridges between the Cu1 nodes. The net is self-penetrating, as highlighted by the blue rod passing through the orange 8-membered shortest circuit. (Reproduced from ref. 25 by permission of The Royal Society of Chemistry.)

protonated extent of benzonate, since the ratio of 4,4′-bpy to benzoate ranges from 1 : 1 to 1 : 2 with the increase of the pH value of the reaction from 5.5 to 7.5. In addition to increasing the ratio of 4,4′-bpy to benzoate in the complexes, pH effect also significantly influences on the tendency of 4,4′-bpy as a bridging ligand. As demonstrated in **1** to **5**, at pH < 6, no 4,4′-bpy ligand functioned as a bridge, while at pH = 6, only one 4,4′-bpy ligand functioned as a bridge. Further increasing the pH to higher than 7.5, all 4,4′-bpy ligands functioned as bridges. Clearly, the observed dimensional disparity is due to the pH effect on the different forms of the carboxylic acid. The different coordination modes also affect the rest of the coordination sphere of individual metal centers, leading to the different ratios of benzoate to 4,4′-bpy observed in the final products.

There also exist a number of examples[25–27] in which although there are no dimensional changes of the architectures at different pH, the detailed structures differ drastically. For example, the reaction of Cu(OAc)$_2$·H$_2$O with H$_4$bptc (H$_4$bptc = 3,3′,4,4′-benzophenonetetra-carboxylic acid) and bpa (bpa = 1,2-bis-(4-pyridy)ethane)[25] at pH = 3 produced {Cu(H$_2$bptc)(bpa)(μ_2-H$_2$O)}$_n$ (**6**), an open 3D rhombic framework based on an

infinite metal-aqua chain (Fig. 6), while at pH = 7, a rather unusual 3D, trinodal, 4-connected self-penetrating network microporous framework formulated as {[Cu$_2$(bptc)(bpa)$_2$(H$_2$O)]·6.5H$_2$O}$_n$ (**7**) was obtained (Fig. 7). Their structural difference originates from the different coordination modes of bptc ligand, a direct consequence of the different degree of protonation of the carboxylato ligand; at pH = 3, the ligands are unidentate, whereas at pH = 7, the they adopt the bridging mode.

The pH influence on the structural variation of certain metal–organic architectures is subtle and intriguing, and a rationalization of the results is admittedly not readily available.[28–33] For example, the reaction of Co(OAc)$_2$·4H$_2$O with 5-*tert*-butyl isophthalic acid (tbip) and 1,3-bi(4-pyridyl)propane (bpp)[28]

produced a one-dimensional tube-like structure of {[Co(tbip)(bpp)(H$_2$O)]$_2$·4H$_2$O}$_n$ (**8**) (Fig. 8) and a two-dimensional corrugated network structure of {[Co(tbip)(bpp)]·H$_2$O}$_n$ (**9**) (Fig. 9) at pH = 6 to 7.5, respectively. In the two compounds, the tbip ligand is fully deprotonated, and the Co–tbip–bpp ratio is the same; the only differences are (1) there are two additional aqua ligands in the lower-pH case and (2) the conformation of the bpp ligands and their relative orientation with respect to the coordination of the Co(II) ions.

In addition to affecting the degree of protonation of the carboxylic acid ligand and therefore their coordination mode, the influence of pH is also reflected in the frequent formation of hydroxo ligand due presumably to the deprotonation of water. For example, the reaction of Cu-(NO$_3$)$_2$·3H$_2$O and H$_3$BTC (trimesic acid)[29] generated a 2D three-fold parallel interpenetrated network of [Cu$_3$(BTC)$_2$-(H$_2$O)$_3$(NH$_3$)$_4$]$_n$·2nH$_2$O (**10**) at pH 8.3 (Fig. 10), whereas at pH 9.2, a 2D bilayer
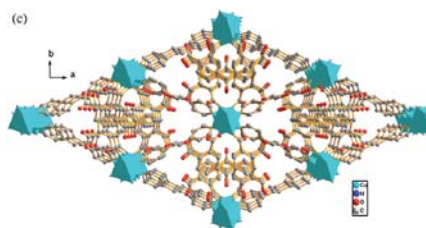

Fig. 6 View of an open rhombic framework based on infinite metal–aqua chain in **6**. (Reproduced from ref. 25 by permission of The Royal Society of Chemistry.)
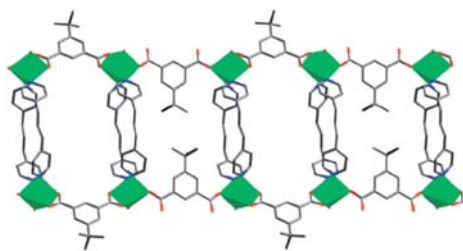
Fig. 8 Side views of a tube-like chain in **8**. (Reprinted with permission from ref. 28. Copyright 2009 The American Chemical Society.)
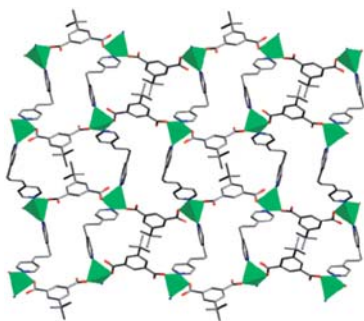
Fig. 9 2D sheets bridged by bpp molecules in **9**. (Reprinted with permission from ref. 28. Copyright 2009 The American Chemical Society.)
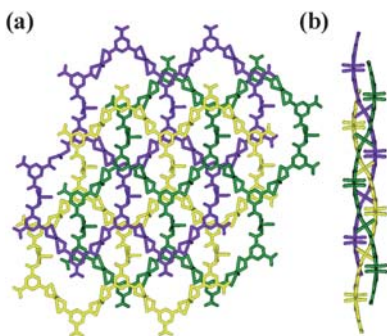
Fig. 10 A perspective view of (a) the three-fold parallel interpenetration network of **10** (the three layers are represented in different colours) and (b) side view of (a). (Reprinted with permission from ref. 29. Copyright 2007 The American Chemical Society.)

structure of $[Cu_4(BTC)_2(OH)_2(H_2O)_2(NH_3)_4]_n$ (**11**) was obtained (Fig. 11). The participation of hydroxo ligands in the coordination of the latter is clearly why the two structures are so different.

## 2.2 pH effect on the structures of polyoxometalates-based metal–organic architectures

Bearing unique properties and exhibiting a diverse compositional range, poly-oxometalates (POMs) represent an attractive class of molecular building

blocks for the construction of supramolecular materials.[34] There are a large number of coordinating atoms in a POM, but their coordinating power is relatively weak because of the diffuse and small amount of negative charge associated with each of these coordinating atoms. As a result, the assembly of POM-based coordination polymers is sensitive to synthesis conditions,[35] analogous to the use of carboxylate ligands. As compared with the extensive use of carboxylate ligands in the construction of metal–organic architectures, the number of POMs-based metal–organic assemblies is rather small. Even so, the profound pH dependence of the final structure has been clearly shown. The coordinating ability of POM may be affected by the pH condition and so resulting in different structures.[36–38] Change in pH may also lead to structural change in the POM itself, and hence the assembly based on these uniquely structured building blocks.[39–41] Metal oxidation numbers may also be altered upon pH change of the reaction mixture containing POM, which in turn, induces structural change of the resulting coordination frameworks.[35]

The pH influence on POM coordinating ability is manifested by the distinctly different structures obtained from the reaction using a mixture of

$Cu(NO_3)_2 \cdot 6H_2O$, silicotungstic acid and 4,4′-bipy under different pH conditions. In the compound of $\{[Cu_2(4,4'-bpy)(4,4'-Hbpy)_4(H_2O)_4](SiW_{12}O_{40})_2(H_2O)_4\}_n$ (**12**) obtained at pH = 3.5, the Keggin anion does not provide any coordination to the Cu(II) ions (Fig. 12).[36] When the pH increased to 5.5, each of the Keggin anions in the compound of $\{[Cu_2(\mu_2-H_2O)_2(4,4'-bpy)_3(SiW_{12}O_{40})](H_2O)_6\}_n$ (**13**) coordinates two Cu(II) ions (Fig. 13). Further increase of pH to 8.5 resulted in each Keggin anion in the compound of $\{[Cu_2(\mu_2-OH)(4,4'-bpy)_3(SiW_{12}O_{40})][Cu_2(\mu_2-O)(4,4'-bpy)_4(H_2O)_2]_{0.5}(H_2O)_4\}_n$ (**14**) coordinating to four Cu(II) ions (Fig. 14). The coordination difference in the Keggin anion at different pH leads to the dimension of the POMs-based architectures from 0D, 2D to 3D.

Structural change of POM units was observed in the reaction of Ni-$(NO_3)_2 \cdot 6H_2O$, $H_4O_{40}SiW_{12}$ and 4,4′-bpy under different pH conditions.[39] At pH = 6, a 2D structure of $[Ni(4,4'-Hbpy)_2(4,4'-bpy)(H_2O)_2](SiW_{12}O_{40}) \cdot 6H_2O$ (**15**) (Fig. 15) was obtained, in which the de-protonated Keggin anion maintains its parent structure. Interestingly, a 1D Z-shaped chain of $[SiW_{11}O_{39}Ni(4,4'-bpy)][Ni(4,4'-Hbpy)_2(H_2O)_2] \cdot (4,4'-H_2bpy) \cdot 6H_2O$ (**16**) (Fig. 16) was formed at pH = 7, wherein one of W atom in the original
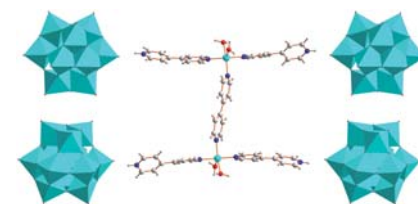

Fig. 12 Plot showing the hydrogen bonding between $SiW_{12}O_{40}^{4-}$ anions and $[Cu_2(4,4'-bpy)(4,4'-Hbpy)_4(H_2O)_4]^{8+}$ unit in **12**.
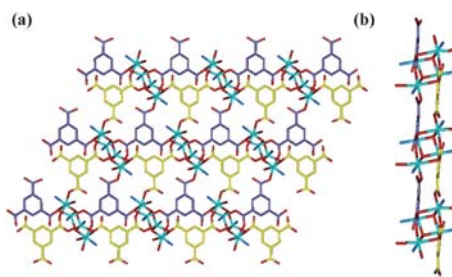

Fig. 11 A perspective view of (a) the bilayer structure of **11** (the three layers are represented in different colours) and (b) side view of (a). (Reprinted with permission from ref. 29. Copyright 2007 The American Chemical Society.)
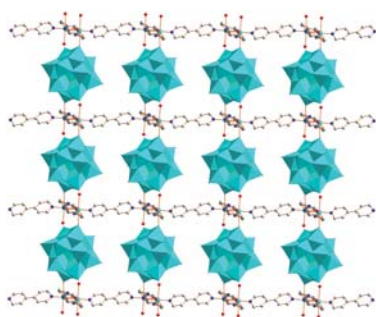
Fig. 13 Plot showing the 2D $[Cu_2(\mu_2\text{-}H_2O)_2(4,4'\text{-bpy})_3(SiW_{12}O_{40})]_n$ in **13** viewed along c axis.
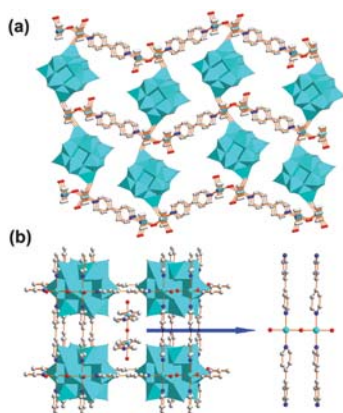
Fig. 14 Plot showing 3D structure of **14** viewed along the c axis (a) and along the b axis (b).
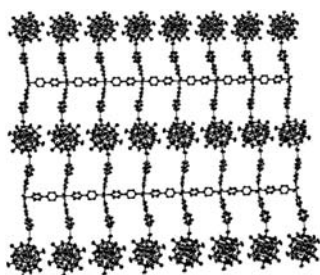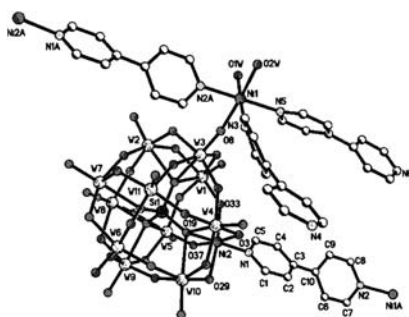

Fig. 15 ORTEP plot showing 2D structure in **15**. Hydrogen atoms were omitted for clarity. (Reprinted with permission from ref. 39 Copyright 2005 The American Chemical Society.)

Keggin anion was replaced by a Ni(II) ion (Fig. 17).

Another interesting example of POM structural change upon pH variation is established by the isomerization of $Mo_7O_{24}{}^{6-}$ anion in the reaction of $(NH_4)_6Mo_7O_{24}\cdot4H_2O$ with bbi (1,1'-(1,4-butanediyl)bis(imidazole)) and Cu-$(NO_3)_2\cdot3H_2O$.[40] At pH 4 to 5, the

Fig. 16 ORTEP plot showing 1D Z-shaped chain in **16**. Hydrogen atoms were omitted for clarity. (Reprinted with permission from ref. 39. Copyright 2005 The American Chemical Society.)

Fig. 17 ORTEP plot showing the $[SiW_{11}O_{39}Ni(4,4'\text{-Hbpy})]$ unit and the coordination environment of Ni(II) ions in **16**. (Reprinted with permission from ref. 39. Copyright 2005 The American Chemical Society.)

$Mo_7O_{24}{}^{6-}$ anion changed into δ-$Mo_8O_{26}{}^{4-}$ and α-$Mo_8O_{26}{}^{4-}$, the resulting product of $[Cu(bbi)]_2[Cu_2(bbi)_2(\delta\text{-}Mo_8O_{26})_{0.5}][\alpha\text{-}Mo_8O_{26}]_{0.5}$ (**17**) exhibits an intricate 3D supramolecular structure (Fig. 18), while at pH = 2, a 2D supramolecular sheet of $[Cu(bbi)(\theta\text{-}Mo_8O_{26})_{0.5}][Cu(bbi)]$ (**18**) was obtained (Fig. 19), in which the original $Mo_7O_{24}{}^{6-}$ anion is transformed into θ-$Mo_8O_{26}{}^{4-}$.

A unique example is provided by the reaction of $H_4SiW_{12}O_{40}$, 4,4'-bpy, and Cu(II) ion.[35] At pH $\sim$ 5, a 3D metal–organic framework of $\{[Cu_2(4,4'\text{-bpy})_4\text{-}(H_2O)_4]\cdot(SiW_{12}O_{40})\cdot(H_2O)_{18}\}_n$ (**19**) was obtained. It can be viewed as adjacent

four-connected 2D structures of $[Cu(4,4'\text{-}bpy)_2(H_2O)_2]_n{}^{2n+}$ being associated through the direct incorporation of the $SiW_{12}O_{40}{}^{4-}$ anion (Fig. 20). At pH $\sim$ 8, a 3D structure of $\{[Cu(4,4'\text{-bpy})_{1.75}]_4(Si\text{-}W_{12}O_{40})(H_2O)_3\}_n$ (**20**) composed of adjacent pseudo-6^3 networks (formed by interlocking adjacent 1D chains of $\{[Cu(4,4'\text{-bpy})_{1.75}]_4\}_n{}^{4n+}$ with hexagonal voids) interpenetrated with $SiW_{12}O_{40}{}^{4-}$ anion was obtained in which the original Cu(II) ion is reduced to Cu(I) (Fig. 21).

## 2.3 pH effect on the structures of imidazole-based metal–organic architectures

The imidazole group, because of its presence in almost all copper proteins, has received great interest both in synthetic models for copper protein active sites[42,43] and in the design of host molecules for the recognition of copper ions.[44,45] Recent studies established the significant role of imidazole-based ligands in the construction of metal–organic architectures.[46] As in the case of carboxylato ligands, the pH condition of a reaction mixture containing imidazole-based ligands determines the degree of protonation of the ligands and therefore their coordination mode, metal to ligand ratio, and the structure of the final products. The reported pH effects on the structure of imidazole-
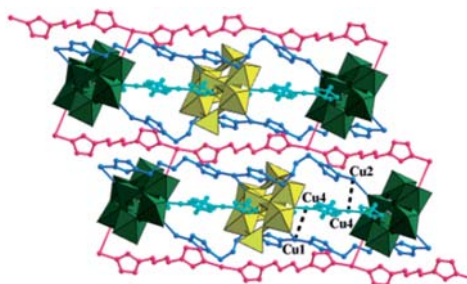
Fig. 18 Ball-and-stick and polyhedral representations of the polythreaded structure in **17**. (Yellow and green polyhedra represent $[\delta\text{-}Mo_8O_{26}]^{4-}$ and $[\alpha\text{-}Mo_8O_{26}]^{4-}$ polyoxoanions, respectively, and black dashed lines represent Cu^I–Cu^I interactions between two $[Cu(bbi)]^+{}_\infty$ chains.) (Reprinted with permission from ref. 40. Copyright 2008 The American Chemical Society.)
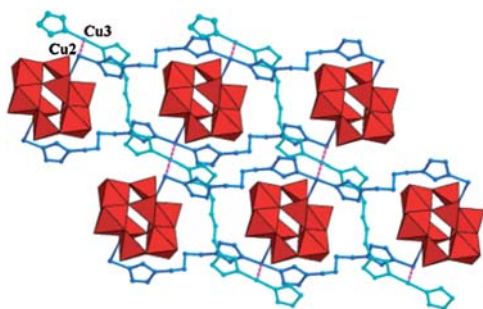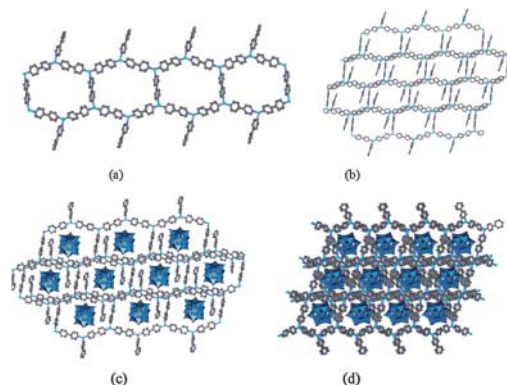
Fig. 19 Ball-and-stick and polyhedral representations of the 2D polythreaded structure in **18**. (Red polyhedra represent [θ-Mo$_8$O$_{26}$]$^{4-}$ polyoxoanions, and pink dashed lines represent Cu^I–Cu^I interactions between two [Cu(bbi)]$^+_\infty$ chains.) (Reprinted with permission from ref. 40. Copyright 2008 The American Chemical Society.)
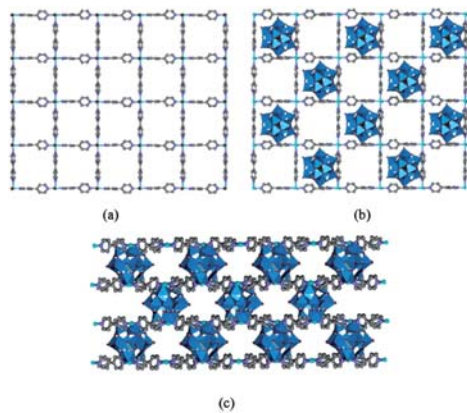
Fig. 20 (a) Structure of the 4^4 network of [Cu(4,4′-bpy)$_2$(H$_2$O)$_2$]$_n^{2+}$ in **19**, (b) arrangement of the SiW$_{12}$O$_{40}$$^{4-}$ anion in the 4^4 network in **19**, and (c) 3D structure of **19** (Cu = cyan; O = red; W = blue; Si = grey; C = grey; N = Cambridge blue). (Reprinted with permission from ref. 35. Copyright 2006 The American Chemical Society.)

Fig. 21 (a) Structure of the 1D chain of {[Cu(4,4′-bpy)$_{1.75}$]$_4$}$_n^{4n+}$ in **20**, (b) structure of the pseudo-6^3 network of [Cu(4,4′-bpy)$_{1.75}$]$_n^{n+}$ in **20**, (c) arrangement of the SiW$_{12}$O$_{40}$$^{4-}$ anion in the 2D network in **20**, and (d) 3D structure of **20** (Cu = cyan; O = red; W = blue; Si = grey; C = grey; N = Cambridge blue). (Reprinted with permission from ref. 35. Copyright 2006 The American Chemical Society.)

based metal–organic architecture are reflected in two aspects, one being the deprotonated ligand resulting in discrete molecular complexes that are further hydrogen-bonded into supramolecular assemblies,[47–49] and the other being the resultant discrete molecular complexes covalently linked into molecular aggregation or coordination polymer.[50–55] As shown in Fig. 22, at a relative low pH, the

reaction of N,N′-bis((2-substituted-imidazol-4-yl)methylene)-3,3′-diaminodipropylamine (2-substituent = H, H$_2$L$_2$) with Cu(ClO$_4$)$_2$ yields a discrete mononuclear complex [Cu(H$_2$L$_2$)]·(ClO$_4$)$_2$ (**21**). At a higher pH, one of the imidazole groups in the ligand was deprotoned, and the adjacent [Cu(HL$_2$)]$^+$ units are self-assembled into a 1D helical chain of {[Cu(HL$_2$)](ClO$_4$)}$_n$ (**22**) via hydrogen bonding interactions.[47]

In addition to the aforementioned hydrogen-bonded assembly, discrete metal complex units formed at a relatively high pH can also be covalently linked, affording a 1D zig-zag chain of **23**[50] (Fig. 23) or a molecular square of ([Cu(HL$_1$)]$^+$)$_4$ (**24**)[50] (Fig. 24).

3 pH effect on the chirality of supramolecular architectures

Chirality is an essential element of life.[56] It also has significant industrial applications.[57] In the past decades, great efforts have been made generate chiral metal–organic architectures, and several synthetic strategies have been successfully developed.[58–61] In the course of these studies, the influence of pH on the chirality of the metal–organic architectures has gradually been recognized. It has been shown that spontaneous resolution of chiral metal–organic architecture can be achieved upon pH adjustment.[46,49,62] Alternatively, individually chiral structure can be generated because of the transformation of ligands from originally being *meso* to racemic.[63–65] Yet another way of inducing chirality, in particular toward the production of homochiral materials is by using pH to control the kinetics of the crystallization of the metal–ligand assembly.[66–69]

An example illustrating spontaneous resolution of chiral metal–organic architecture is the reaction of tris[2-(((imidazol-4-yl)methylidene)amino)ethyl]amine (H$_3$L^6) with Co(ClO$_4$)$_2$.[49] At a relatively high pH, the complex units [Co(L^6)], formed with the fully deprotonated ligand, are connected by water molecules, leading to a hydrogen-bonded network structure with coexisting C and A enantiomers. At a lower pH, the formal hemi-deprotonated species [Co(H$_{1.5}$L^6)]$^{1.5+}$ self-assembled into an extended 2D homochiral layer structure of
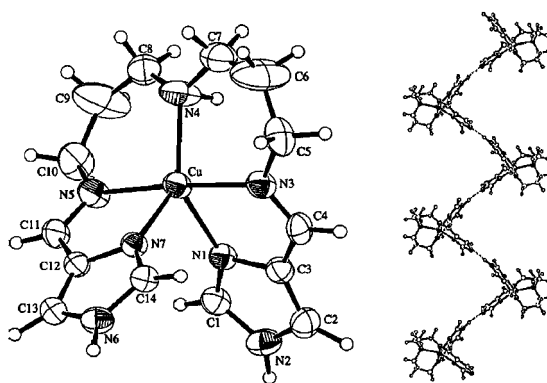
Fig. 22 ORTEP drawing of the cation $[Cu(H_2L_2)]^{2+}$ in **21** (left) and 1D helical chain of $([Cu(HL_2)]^+)_n$ (right) in **22**. (Reprinted with permission from ref. 47. Copyright 1997 The American Chemical Society.)
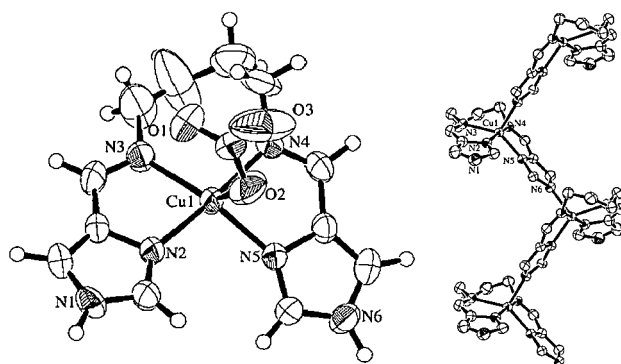
Fig. 23 ORTEP drawing of the cation $[Cu(H_2L_2)]^{2+}$ (left) and 1D zig-zag chain of $([Cu(HL_2)]^+)_n$ (right) in **23**. (Reprinted with permission from ref. 50. Copyright 1998 The American Chemical Society.)
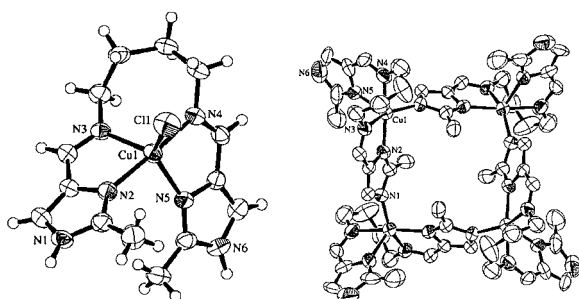
Fig. 24 ORTEP drawing showing the structure of the cation $[Cu(H_2L_1)]^{2+}$ (left) and molecular square of **24** (right) in, (H_2L_1 = bis((2-methyl-imidazol-4-yl)methylene)-3,3′-diaminodi-propyl-amine). (Reprinted with permission from ref. 50. Copyright 1998 The American Chemical Society.)

$\{[Co(H_{1.5}L^6)]^{1.5+}\}_n$ (**25**) containing only one of the enantiomeric forms (Fig. 25).

The influence of pH on the production of chiral metal–ligand assemblies can be appreciated by the outcome of the reaction of $Zn(NO_3)_2·6H_2O$ with $(2S,3S,4R,5R)$-H_4L (H_4L = tetrahydrofurantetracarboxylic acid) in the presence of 1,10-phenanthroline (phen).[63] At pH = 2.0, the 1D structure of $[Zn_2\{(2S,3S,4R,5R)$-L$\}(phen)_2(H_2O)]$·$2H_2O$ (**26**) was obtained, in which the original $2S,3S,4R,5R$ configuration of the ligand is maintained (Fig. 26). At pH = 2.5, the 2D layer structure of $[Zn_4\{(2S,3R,4R,5R)$-L$\}\{(2S,3S,4S,5R)$-L$\}$-$(phen)_2(H_2O)_2]$ (**27**) is obtained in wherein the initial *meso*-L ligands are now present as an enatiomeric pair, $(2S,3R,4R,5R)$- and $(2S,3S,4S,5R)$-L (Fig. 26).

The ability to control the crystallisation kinetics aiming at the creating of one particular chiral form of metal–ligand assembly has recently been demonstrated by the control of reaction pH of the reaction of $Cu(NO_3)_2$ with 4,4′-bpy and succinate.[66] Despite the fact that every coordination polymer chain of Cu(succinate) in the 3D network of $[\{Cu(succinate)(4,4′-bpy)\}_n]·(4H_2O)_n$ (**28**) (Fig. 27) is helical and inherently chiral, the equal probability of forming the two enantiomeric forms means that the bulk material is a racemic conglomerate and not optically active. Consistent are the CD-silent (Fig. 28) samples obtained upon quick crystallization at pH 8.4. Adding ammonia to the reaction caused complexation of Cu(II) ion, in competition with its coordination with the succinato ligand; as the pH of the reaction was gradually increased, Cu(II) was slowly released and the crystallization of the corresponding Cu(II)-succinate coordination polymer was controlled. In the extreme case of one crystallization event, the sole single crystal must be in one of the enantiomeric forms, present in 100%. This is the case when the pH of the reaction mixture was raised to 9.2; out of the 30 crystallisations investigated, all of them are CD active (Fig. 29), demonstrating that chiral symmetry breaking was achieved. Corroborating is the somewhat active CD spectra of the sample when the pH was 8.7; the sample is somewhat CD active in the bulk (Fig. 30).

4 pH effect on the *in situ* synthesis of metal/ligand reactions

In situ synthesis of organic ligands, often under hydro(solvo)thermal conditions in the presence of presumably catalytic metal ions, and the subsequent metal coordination chemistry are important research topics in both coordination chemistry and synthetic organic chemistry.[70] More than 10 general types of *in situ* transformation of organic ligands have been reported, including hydroxylation,[71] alkylation,[72] carbon–carbon bond formation,[73] hydrolysis,[74] tetrazole and triazole formation,[75] acylation[76] and others.[77] We provide here only two examples of how pH conditions affect the outcome of the *in situ* ligand synthesis and
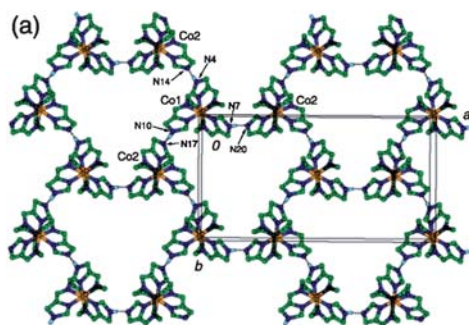
Fig. 25 Top view showing the layer structure of **25**, in which the same enantiomers (C = green) are linked by intermolecular imidazole–imidazolate hydrogen bonds. (Reprinted with permission from ref. 49. Copyright 2002 The American Chemical Society.)
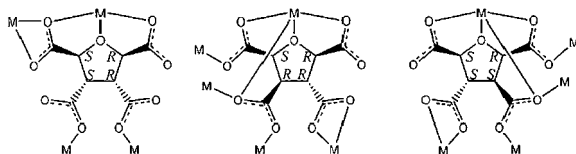
Fig. 26 Configurations and coordination modes of L ligands in **26** and **27**. (Reprinted with permission from ref. 63. Copyright 2009 WILEY-VCH.)
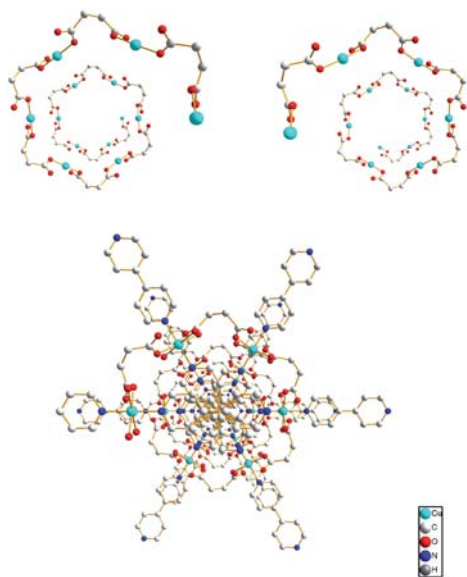
Fig. 27 ORTEP plot showing with thermal ellipsoids set at the 30% probability level showing the right-handed helix of polymeric [{Cu(succinate)}$_n$] (up, left), the left-handed helix of polymeric [{Cu(succinate)}$_n$] (up, right), and the overall structure of **28** (down) viewed along the c axis. (Reprinted with permission from ref. 66. Copyright 2007 WILEY-VCH.)

metal coordination of the resulting ligands. Interested readers are referred to two comprehensive reviews[71] that are dedicated to detailed discussions of *in situ* ligand synthesis and metal complexation.

The reaction using a mixture of Cu(NO$_3$)$_2$, 1,2,3-btcH3 (1,2,3-btcH3 = 1,2,3-benzenetricarboxylic acid) and 4,4′-bpy[78] produced in the absence of NaOH a 3D network {[Cu$_2$(1,2,3-btc)(4,4′-bpy)(H$_2$O)$_2$](NO$_3$)}$_n$ (**29**) wherein the tricarboxylic acid ligand maintains its original form (Fig. 31). With the addition of 2 equiv. NaOH to the reaction mixture, a 3,4-connected 2D network of [Cu$_2$(ip)(ipH)(4,4′-bpy)$_{1.5}$]$_n$ (**30**) (Fig. 32) was obtained, and the btc ligand has now been transformed into isophthalate (ip).

Further increase of the amount of NaOH to 4 equiv. resulted in the assembly of [Cu$_3$(ipO)$_2$(4,4′-bpy)$_{0.5}$(H$_2$O)$_2$]$_n$ (**31**), a 2D network (Fig. 33) featuring 2-hydroxyisophthalate (ipO) transformed from 1,2,3-btcH$_3$. The *in situ* ligand transformation is conveniently summarised in Fig. 34.

The second example involves the use of iminodiacetic acid (INA) in the hydrothermal synthesis of its lanthanide complexes.[79,80] A mixture containing iminodiacetic acid and Ln$_2$O$_3$ at pH *ca.* 1 produced 2,5-dioxopiperazine-1,4-diacetic (**32**) (Fig. 35), a product formally generated by a pair of intermolecular condensation reaction between one of the carboxylic groups of one INA and the amino group of the second INA, whereas while at pH *ca.* 4, some of the ligand was transformed into oxalate, co-existing with the undecomposed INA ligand. Not surprisingly, different 3D metal–organic architectures of [Dy$_2$(ox)$_2$L(H$_2$O)$_2$]$_n$ (L = 2,5-diketopiperazine-1,4-diacetate, ox = oxalate) (**33**) and {[Dy$_2$(ox)$_2$Ni(IDA)$_2$-(H$_2$O)$_2$]}$_n$·2nH$_2$O (**34**) were obtained under these different pH conditions, and their structures are shown in Fig. 36 and Fig. 37, respectively.

5 Summary and outlook

In this *Highlight* the interesting and often surprising results from recent studies of pH effects on the assembly of metal–organic architectures are summarized. This *Highlight* only attempts to illustrate the key effects observed when the pH condition of the reaction varies, and is not intended to be a comprehensive survey of studies where pH effects are involved.[81–84] Thus, only certain selected yet representative ligand systems (carboxylate, POM, imidazole-based) are chosen for the demonstration of the pH influences, which include pH-dependent ligand forms, the generation and metal coordination of hydroxides, *in situ* ligand transformation to different kinds, and the control of crystallization kinetics. It is clearly that pH condition plays an important role in determining the final structures of the metal–organic architectures. Notwithstanding the progresses that have been made recently, it appears that predicting any specific effects caused by pH change remains an inexact practice as not only such effects are not known
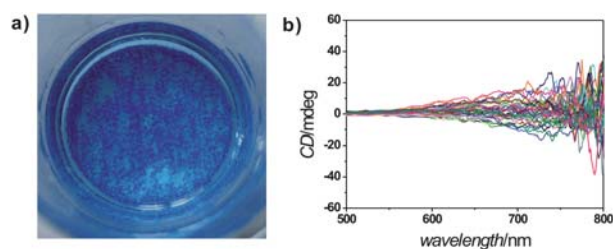
Fig. 28 Crystallization using pH 8.3 solutions. (a) A rapid crystallization of **28** yielding a large number of small crystals. (b) The solid-state CD spectra of bulk samples of 30 different crystallisations. (Reprinted with permission from ref. 66. Copyright 2007 WILEY-VCH.)
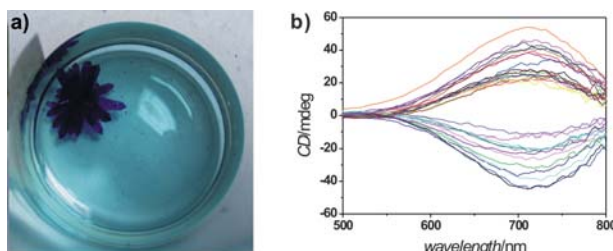
Fig. 29 Crystallization using pH 9.2 solutions. (a) The production of a small number of crystal clusters of **28** with slow evaporation of the reaction mixture. (b) The soli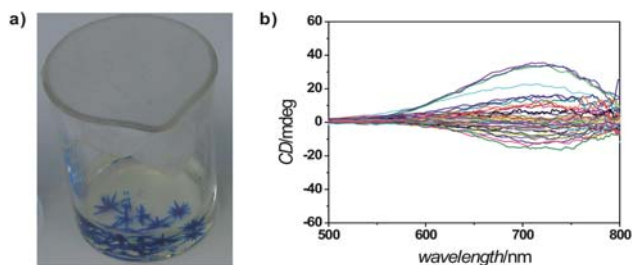d-state CD spectra of bulk samples from 30 different slow crystallisations. The positive and negative values correspond to the right- and left-handed helices, respectively. (Reprinted with permission from ref. 66. Copyright 2007 WILEY-VCH.)
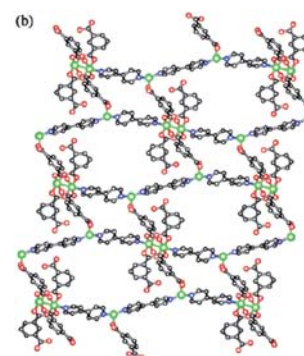

Fig. 30 Crystallization using pH 8.7 solutions. (a) The production of a relatively small number of crystal clusters of **28** with slow evaporation of the reaction mixture. (b) The solid-state CD spectra of bulk samples from 30 different crystallisations. The positive and negative values correspond to the right- and left-handed helices, respectively. (Reprinted with permission from ref. 63. Copyright 2007 WILEY-VCH.)
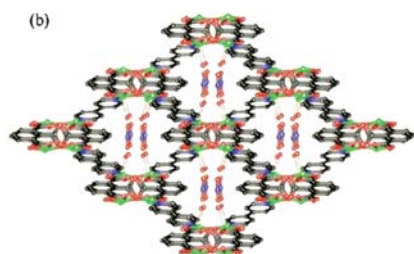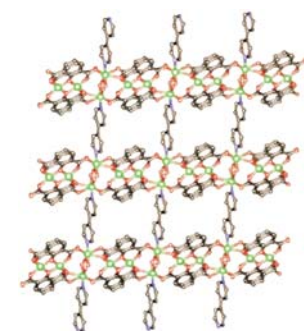

Fig. 31 Perspective views of the 3D network of **29**. (Reproduced from ref. 78 by permission of The Royal Society of Chemistry (RSC) for the Centre National de la Recherche Scientifique (CNRS) and the RSC.)

Fig. 32 Perspective views of the 2D network of **30**. (Reproduced from ref. 78 by permission of The Royal Society of Chemistry (RSC) for the Centre National de la Recherche Scientifique (CNRS) and the RSC.)

Fig. 33 Perspective views of the 2D network of **31**. (Reproduced from ref. 78 by permission of The Royal Society of Chemistry (RSC) for the Centre National de la Recherche Scientifique (CNRS) and the RSC.)

a priori, there is often more than one effect that comes into play, leading to complex and diverse structures of the metal–organic assemblies. Furthermore, the assembly of the solid state structures of such architectures is governed by a number of intermolecular forces in addition to the pH influence. Frequently the balance between these different forces are so subtle that an explanation of certain structures observed is admittedly not yet available. For example, the reasons for the generation of structural isomers using the same mixture of $Co(OAc)_2 \cdot 4H_2O$, 5-*tert*-butyl isophthalic

acid (tbip) and 1,3-bi(4-pyridyl)propane (bpp) at different pH conditions,[28] the spontaneous resolution of chiral metal–organic architecture as demonstrated in the reaction of tris[2-(((imidazol-4-yl)-methylidene)amino)ethyl]amine with $Co(ClO_4)_2$, and the *in situ* formation of the two different types of ligands in the reaction of $Cu(NO_3)_2$ with 1,2,3-btcH3 and 4,4′-bipy[78] are unclear[49]

Another example of particular note is the formation of two closely related crystal structures by the reaction of 1,3-bis(5-methylimidazol-4-ylmethyleneimino)-propan-2-ol (H₂BIPO) with Cu(II) ion.[46] These two metal–organic architectures, shown in Fig. 38, have the same formula and identical individual chain structure. However, one crystallized in the centro-symmetric space group $P2_1/n$ with its adjacent helical chains packed in opposite directions, whereas the other crystallised in the chiral space groups ($P2_1$) and the
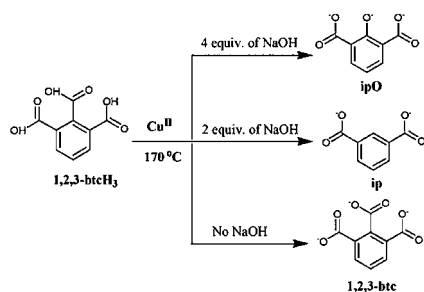
Fig. 34 Fate of 1,2,3-btcH3 in media with different equivalents of NaOH. (Reproduced from ref. 78 by permission of The Royal Society of Chemistry (RSC) for the Centre National de la Recherche Scientifique (CNRS) and the RSC.)
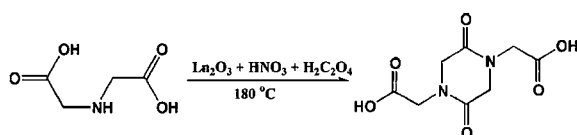

Fig. 35 Schematic view of hydrothermal *in situ* generation of **32**.
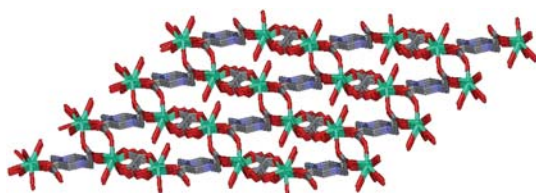
Fig. 36 Stick plot showing the 3D structure of **33**.
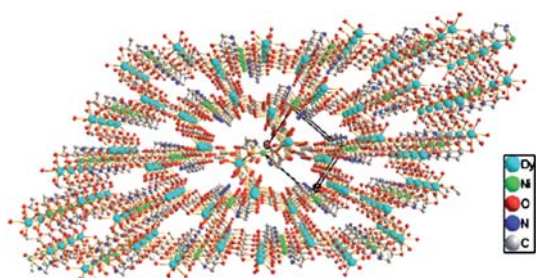
Fig. 37 Ball and stick plot showing the 3D structure of **34**.
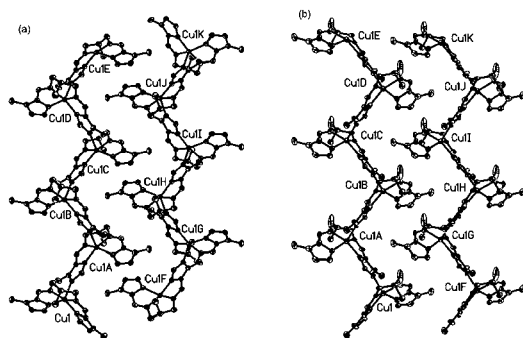
Fig. 38 (a) Two adjacent helical chains arranged in opposite directions in {[Cu(HBIPO)]-ClO$_4$·H$_2$O}$_n$. (b) All adjacent helical chains arranged in the same direction in {[Cu(HBIPO)]-ClO$_4$·H$_2$O}$_n$.

chains are arranged in the same direction (Fig. 38).

Further progress and a better understanding of the diverse effects of pH condition depend on more systematic studies, for example, by using the same ligand system. Mechanistic studies aiming at discerning the individual and specific contributions of various effects appears to be critical also. For example, isolation of any possible intermediates should provide insight into at which particular step the effect comes into play. Probably most needed at this stage are the computational studies, essentially none at this point, of the often energetically close systems due to the pH effects. Combined, the experimental and computational studies will reward us with a better understanding of such effects and the ability to manipulate them in the context of crystal engineering for the making of structurally sophisticated and functionally stimulating materials.

Acknowledgements

References

1 R. Pepinsky, *Phys. Rev.*, 1955, **100**, 971.
2 G. R. Desiraju, *Crystal engineering: The design of organic solids*, Elsevier, Amsterdam.
3 N. Champness, *CrystEngComm*, 2007, **9**, 437–437; V. R. Thalladi, B. S. Goud, V. J. Hoy, F. H. Allen, J. A. K. Howard and G. R. Desiraju, *Chem. Commun.*, 1996, 401–402.
4 C. Janiak, *J. Chem. Soc., Dalton Trans.*, 2000, 3885–3896; T. Kawase and H. Kurata, *Chem. Rev.*, 2006, **106**, 5250–5273.
5 P. Metrangolo, H. Neukirch, T. Pilati and G. Resnati, *Acc. Chem. Res.*, 2005, **38**, 386–395; R. B. Walsh, C. W. Padgett, P. Metrangolo, G. Resnati, T. W. Hanks and W. T. Pennington, *Cryst. Growth Des.*, 2001, **1**, 165–175; B. K. Saha, A. Nangia and M. Jaskólski, *CrystEngComm*, 2005, **7**, 355–358; P. Metrangolo and G. Resnati, *Chem.–Eur. J.*, 2001, **7**, 2511–2519; T. Caronna, R. Liantonio, T. A. Logothetis, P. Metrangolo, T. Pilati and G. Resnati, *J. Am. Chem. Soc.*, 2004, **126**, 4500–4501.
6 D. B. Leznoff, B.-Y. Xue, R. J. Batchelor, F. W. B. Einstein and B. O. Patrick, *Inorg.*

Chem., 2001, **40**, 6026–6034; E. J. Fernández, M. C. Gimeno, A. Laguna, J. M. López-de-Luzuriaga, M. Monge, P. Pyykkö and D. Sundholm, *J. Am. Chem. Soc.*, 2000, **122**, 7287–7293; M. A. Rawashdeh-Omary, M. A. Omary, H. H. Patterson and J. P. Fackler, Jr., *J. Am. Chem. Soc.*, 2001, **123**, 11237–11247.

7 F. Corbellini, R. Fiammengo, P. Timmerman, M. Crego-Calama, K. Versluis, A. J. R. Heck, I. Luyten and D. N. Reinhoudt, *J. Am. Chem. Soc.*, 2002, **124**, 6569–6575; F. Corbellini, L. D. Costanzo, M. Crego-Calama, S. Geremia and D. N. Reinhoudt, *J. Am. Chem. Soc.*, 2003, **125**, 9946–9947; Y. Chi and S. H. Gellman, *J. Am. Chem. Soc.*, 2006, **128**, 6804–6805.

8 G. R. Desiraju, *Acc. Chem. Res.*, 2002, **35**, 565–573; G. R. Desiraju, *Chem. Commun.*, 2005, 2995–3001; D. Braga and F. Grepioni, *Acc. Chem. Res.*, 2000, **33**, 601–608; L. Brammer, *Chem. Soc. Rev.*, 2004, **33**, 476–489; B. Moulton and M. J. Zaworotko, *Chem. Rev.*, 2001, **101**, 1629–1658; H. W. Roesky and M. Andruh, *Coord. Chem. Rev.*, 2003, **236**, 91–119.

9 B. Zheng, H. Dong, J. F. Bai, Y. Z. Li, S. H. Li and M. Scheer, *J. Am. Chem. Soc.*, 2008, **130**, 7778–7779; S. Khatua, T. Harada, R. Kurodabc and M. Bhattacharjee, *Chem. Commun.*, 2007, 3927–3929; R. Yamasaki, A. Tanatani, I. Azumaya, H. Masu, K. Yamaguchi and H. Kagechika, *Cryst. Growth Des.*, 2006, **6**, 2007–2010; V. R. Pedireddi and S. Varughese, *Inorg. Chem.*, 2004, **43**, 450–457; T. Wu, D. Li and S. W. Ng, *CrystEngComm*, 2005, **7**, 514–518.

10 M.-L. Tong, S. Hu, J. Wang, S. Kitagawa and S. W. Ng, *Cryst. Growth Des.*, 2005, **5**, 837–839; J. X. Chen, M. Ohba, D. Zhao, W. Kaneko and S. Kitagawa, *Cryst. Growth Des.*, 2006, **6**, 664–668; D. F. Sun, Y. X. Ke, T. M. Mattox, B. A. Ooro and H.-C. Zhou, *Chem. Commun.*, 2005, 5447–5449; Y.-B. Dong, Y.-Y. Jiang, J. Li, J.-P. Ma, F.-L. Liu, B. Tang, R.-Q. Huang and S. R. Batten, *J. Am. Chem. Soc.*, 2007, **129**, 4520–4521.

11 M. Tsaramyrsi, M. Kaliva, A. Salifoglou, C. P. Raptopoulou, A. Terzis, V. Tangoulis and J. Giapintzakis, *Inorg. Chem.*, 2001, **40**, 5772–5779; S. Faulkner and B. P. Burton-Pye, *Chem. Commun.*, 2005, 259–261.

12 (*a*) P. M. Forster, N. Stock and A. K. Cheetham, *Angew. Chem., Int. Ed.*, 2005, **44**, 7608–7611; (*b*) S. Bauer, T. Bein and N. Stock, *Inorg. Chem.*, 2005, **44**, 5882–5889; (*c*) N. Stock and T. Bein, *Angew. Chem., Int. Ed.*, 2004, **43**, 749–752; (*d*) T. Poon, J. Sivaguru, R. Franz, S. Jockusch, C. Martinez, I. Washington, W. Adam, Y. Inoue and N. J. Turro, *J. Am. Chem. Soc.*, 2004, **126**, 10498–10499; (*e*) M. Casarin, C. Corvaja, C. D. Nicola, D. Falcomer and L. Franco, *Inorg. Chem.*, 2005, **44**, 6265–6276.

13 B. J. Holliday and C. A. Mirkin, *Angew. Chem., Int. Ed.*, 2001, **40**, 2022–2043.

14 S. T. Wu, L. S. Long, R. B. Huang and L. S. Zheng, *Cryst. Growth Des.*, 2007, **7**, 1746–1752.

15 Q. Yu, X. Q. Zhang, H. D. Bian, H. Liang, B. Zhao, S. P. Yan and D. Z. Liao, *Cryst. Growth Des.*, 2008, **8**, 1140–1146.

16 C.-C. Wang, C.-H. Yang and G.-H. Lee, *Eur. J. Inorg. Chem.*, 2006, 820–826.

17 H. J. Chen and X. M. Chen, *Inorg. Chim. Acta*, 2002, **329**, 13–21.

18 Y. F. Zhou, B. Y. Lou, D. Q. Yuan, Y. Q. Xu, F. L. Jiang and M. C. Hong, *Inorg. Chim. Acta*, 2005, **358**, 3057–3064.

19 C. Y. Fang, Z. X. Chen, X. F. Liu, Y. T. Yang, M. L. Deng, L. H. Weng, Y. Jia and Y. M. Zhou, *Inorg. Chim. Acta*, 2009, **362**, 2101–2107.

20 W. Wu and J. M. Xie, *J. Coord. Chem.*, 2008, **61**, 2288–2295.

21 F. T. Xie, H. Y. Bie, L. M. Duan, G. H. Li, X. Zhang and J. Q. Xu, *J. Solid State Chem.*, 2005, **178**, 2858–2866.

22 G. C. Ou, C. Y. Su, J. H. Yao and T. B. Lu, *Inorg. Chem. Commun.*, 2005, **8**, 421–424.

23 Q. Chu, G. X. Liu, T.-A. Okamura, Y. Q. Huang, W. Y. Sun and N. Ueyama, *Polyhedron*, 2008, **27**, 812–820.

24 A. Roth, A. Buchholz and W. Plass, *Z. Anorg. Allg. Chem.*, 2007, **633**, 383–392.

25 H. Wang, Y.-Y. Wang, G.-P. Yang, C.-J. Wang, G.-L. Wen, Q.-Z. Shia and S. R. Batten, *CrystEngComm*, 2008, **10**, 1583–1594.

26 R. Q. Zhong, R. Q. Zou, M. Du, T. Yamada, G. Maruta, S. Takedac and Q. Xu, *Dalton Trans.*, 2008, 2346–2354.

27 J. J. Wang, L. Gou, H. M. Hu, Z. X. Han, D. S. Li, G. L. Xue, M. L. Yang and Q. Z. Shi, *Cryst. Growth Des.*, 2007, **7**, 1514–1521.

28 L. F. Ma, L. Y. Wang, D. H. Lu, S. R. Batten and J. G. Wang, *Cryst. Growth Des.*, 2009, **9**, 1741–1749.

29 W. X. Chen, S. T. Wu, L. S. Long, R. B. Huang and L. S. Zheng, *Cryst. Growth Des.*, 2007, **7**, 1171–1175.

30 Y. B. Go, X. Q. Wang, E. V. Anokhina and A. J. Jacobson, *Inorg. Chem.*, 2004, **43**, 5360–5367.

31 Y. B. Go, X. Q. Wang, E. V. Anokhina and A. J. Jacobson, *Inorg. Chem.*, 2005, **44**, 8265–8271.

32 S. R. Choudhury, A. D. Jana, E. Colacio, H. M. Lee, G. Mostafa and S. Mukhopadhyay, *Cryst. Growth Des.*, 2007, **7**, 212–214.

33 P. K. Chen, Y. X. Che, Y. M. Li and J. M. Zheng, *J. Solid State Chem.*, 2006, **179**, 2656–2662.

34 C. L. Hill, *Chem. Rev.*, 1998, **98**, 1, special issue on POMs.

35 X. J. Kong, Y. P. Ren, P. Q. Zheng, Y. X. Long, L. S. Long, R. B. Huang and L. S. Zheng, *Inorg. Chem.*, 2006, **45**, 10702–10711.

36 F. Yu, X. J. Kong, Y. Y. Zheng, Y. P. Ren, L. S. Long, R. B. Huang and L. S. Zheng, *Dalton Trans.*, 2009, 9503–9509.

37 F. X. Meng, Y. G. Chen, H. B. Liu, H. J. Pang, D. M. Shi and Y. Sun, *J. Mol. Struct.*, 2007, **837**, 224–230.

38 Y. Q. Lan, S. L. Li, X. L. Wang, K. Z. Shao, D. Y. Du, H. Y. Zang and Z. M. Su, *Inorg. Chem.*, 2008, **47**, 8179–8187.

39 P. Q. Zheng, Y. P. Ren, L. S. Long, R. B. Huang and L. S. Zheng, *Inorg. Chem.*, 2005, **44**, 1190–1192.

40 Y. Q. Lan, S. L. Li, X. L. Wang, K. Z. Shao, Z. M. Su and E. B. Wang, *Inorg. Chem.*, 2008, **47**, 529–534.

41 S. Reinoso, M. H. Dickman, M. Reicke and U. Kortz, *Inorg. Chem.*, 2006, **45**, 9014–9019.

42 E. I. Solomon, B. L. Hemming and D. E. Root, in *Bioinorganic Chemistry of Copper*, ed. K. D. Kailin and Z. Tyelar, Chapman & Hall, London, 1993; *Metal Ions in Biological Systems*, ed. H. Sigel, Marcel Dekker Inc., New York, 1981.

43 N. Kitajima and Y. Mora-oka, *Chem. Rev.*, 1994, **94**, 737–757.

44 P. M. Van Berkel, W. L. Driessen, G. J. A. A. Koolhass, J. Reedijk and D. C. Sherrington, *J. Chem. Soc., Chem. Commun.*, 1995, 147–148.

45 G. J. A. A. Koolhass, P. M. Van Berkel, S. C. Van der Slot, G. Mendoza-Diaz, W. L. Driessen, J. Reedijk, H. Kooijman, N. Veldman and A. L. Spek, *Inorg. Chem.*, 1996, **35**, 3525–3532.

46 L. S. Long, J. W. Cai, Y. P. Ren, Y. X. Tong, X. M. Chen, L. N. Ji, R. B. Huang and L. S. Zheng, *J. Chem. Soc., Dalton Trans.*, 2001, 845–849.

47 H. Miyasaka, S. Okamura, T. Nakashima and N. Matsumoto, *Inorg. Chem.*, 1997, **36**, 4329–4335.

48 Y. Shii, Y. Motoda, T. Matsuo, F. Kai, T. Nakashima, J.-P. Tuchagues and N. Matsumoto, *Inorg. Chem.*, 1999, **38**, 3513–3522.

49 I. Katsuki, Y. Motoda, Y. Sunatsuki, N. Matsumoto, T. Nakashima and M. Kojima, *J. Am. Chem. Soc.*, 2002, **124**, 629–640.

50 M. Mimura, T. Matsuo, T. Nakashima and N. Matsumoto, *Inorg. Chem.*, 1998, **37**, 3553–3560.

51 Y. B. Lu, M. S. Wang, W. W. Zhou, G. Xu, G. C. Guo and J. S. Huang, *Inorg. Chem.*, 2008, **47**, 8935–8942.

52 N. Matsumoto, Y. Mizuguchi, G. Mago, S. Eguchi, H. Miyasaka, T. Nakashima and J.-P. Tuchagues, *Angew. Chem., Int. Ed. Engl.*, 1997, **36**, 1860–1862.

53 J. M. Dominguez-Vera, F. Camara, J. M. Moreno, E. Colacio and H. Stoeckli-Evans, *Inorg. Chem.*, 1998, **37**, 3046–3050.

54 Y. Lu, X. H. Lu, Y. Q. Huang, T.-A. Okamura, L. Y. Kong, W. Y. Sun and N. Ueyama, *Z. Anorg. Allg. Chem.*, 2008, **634**, 708–713.

55 X. P. Li, J. Y. Zhang, M. Pan, S. R. Zheng, Y. Liu and C. Y. Su, *Inorg. Chem.*, 2007, **46**, 4617–4625.

56 W. A. Bonner, *Top. Stereochem.*, 1988, **18**, 1–96; L. Q. Keszthelyi, *Q. Rev. Biophys.*, 1995, **28**, 473–507.

57 J. Zyss, *Molecular Nonlinear Optics: Materials, Physics, and Devices*, Academic Press, New York, 1993; F. Agullo-Lopez, J. M. Cabrera, F. Agullo-Rueda, *Electrooptics: Phenomena, Materials and Applications*, Academic Press, New York, 1994; R. E. Newnham, *Structure-Property Relations*, Springer, New York, 1975; G. R. Desiraju, *Crystal Engineering: The Design of Organic Solids*, Elsevier, New

York, 1989; J.-L. Lehn, *Supramolecular Chemistry: Concepts and Perspectives*, VCH, New York, 1995.

58 Y. T. Wang, M. L. Tong, H. H. Fan, H. Z. Wang and X. M. Chen, *Dalton Trans.*, 2005, 424–426; Z. Z. Lin, F. L. Jiang, L. Chen, D. Q. Yuan and M. C. Hong, *Inorg. Chem.*, 2005, **44**, 73–76.

59 E. Q. Gao, Y. F. Yue, S. Q. Bai, Z. He and C. H. Yan, *J. Am. Chem. Soc.*, 2004, **126**, 1419–1429.

60 W. Yuan and L. S. Long, *Appl. Organomet. Chem.*, 2003, **17**, 257–258.

61 D. C. Fox, A. T. Fiedler, H. L. Halfen, T. C. Brunold and J. A. Halfen, *J. Am. Chem. Soc.*, 2004, **126**, 7627–7638; K. M. A. Malik and P. D. Newman, *Dalton Trans.*, 2003, 3516–3525.

62 J. Kühnert, I. Císařová, M. Lamač and P. Štěpnička, *Dalton Trans.*, 2008, 2454–2464.

63 L. Zhang, J. Zhang, Z. J. Li, Y. Y. Qin, Q. P. Lin and Y. G. Yao, *Chem.–Eur. J.*, 2009, **15**, 989–1000.

64 K. D. Demadis, M. Papadaki, R. G. Raptis and H. Zhao, *Chem. Mater.*, 2008, **20**, 4835–4846.

65 K. P. Rao, A. Thirumurugan and C. N. R. Rao, *Chem.–Eur. J.*, 2007, **13**, 3193–3201; H. Kumagai, M. Akita-Tanaka, K. Inoue, K. Takahashi, H. Kobayashi, S. Vilminot and M. Kurmoo, *Inorg. Chem.*, 2007, **46**, 5949–5956; A. J. Bailey, C. Lee, R. K. Feller, J. B. Orton, C. Mellot-Draznieks, B. Slater, W. T. A. Harrison, P. Simoncic, A. Navrotsky, M. C. Grossel and A. K. Cheetham, *Angew. Chem., Int. Ed.*, 2008, **47**, 8634–8637; J. Wang, Z. J. Lin, Y. C. Ou, Y. Shen, R. Herchel and M. L. Tong, *Chem.–Eur. J.*, 2008, **14**, 7218–7235(*a*) J. Wang, Y. H. Zhang and M. L. Tong, *Chem. Commun.*, 2006, 3166–3168.

66 S. T. Wu, Y. R. Wu, Q. Q. Kang, H. Zhang, L. S. Long, Z. P. Zheng, R. B. Huang and L. S. Zheng, *Angew. Chem., Int. Ed.*, 2007, **46**, 8475–8479.

67 R. W. Saalfrank, H. Maid, A. Scheurer, F. W. Heinemann, R. Puchta, W. Bauer, D. Stern and D. Stalke, *Angew. Chem., Int. Ed.*, 2008, **47**, 8941–8945.

68 H. Q. Hao, W. T. Liu, W. Tan, Z. J. Lin and M. Liang Tong, *Cryst. Growth Des.*, 2009, **9**, 457–465.

69 H. Q. Hao, W. T. Liu, W. Tan, Z. J. Lin and M. Liang Tong, *CrystEngComm*, 2009, **11**, 967–971.

70 X. M. Chen and M. L. Tong, *Acc. Chem. Res.*, 2007, **40**, 162–170; X. M. Zhang, *Coord. Chem. Rev.*, 2005, **249**, 1201–1219.

71 S. Hu, J.-C. Chen, M.-L. Tong, B. Wang, Y.-X. Yan and S. R. Batten, *Angew. Chem., Int. Ed.*, 2005, **44**, 5471–5475; J. Tao, Y. Zhang, M.-L. Tong, X.-M. Chen, T. Yuen, C. L. Lin, X. Huang and J. Li, *Chem. Commun.*, 2002, 1342–1343; S. Y. Yang, L. S. Long, R. B. Huang, L. S. Zheng and S. W. Ng, *Inorg. Chim. Acta*, 2005, **358**, 1882–1886.

72 J.-K. Cheng, Y.-G. Yao, J. Zhang, Z.-J. Li, Z.-W. Cai, X.-Y. Zhang, Z.-N. Chen, Y.-B. Chen, Y. Kang, Y.-Y. Qin and Y.-H. Wen, *J. Am. Chem. Soc.*, 2004, **126**, 7796–7797; O. R. Evans and W. Lin, *Cryst. Growth Des.*, 2001, **1**, 9–11.

73 A. J. Blake, N. R. Champness, S. S. M. Chung, W.-S. Li and M. Schröder, *Chem. Commun.*, 1997, 1675–1676; C.-M. Liu, S. Gao and H.-Z. Kou, *Chem. Commun.*, 2001, 1670–1671; N. Zheng, X. Bu and P. Feng, *J. Am. Chem. Soc.*, 2002, **124**, 9688–9689; Q.-H. Wei, L.-Y. Zhang, G.-Q. Yin, L.-X. Shi and Z.-N. Chen, *J. Am. Chem. Soc.*, 2004, **126**, 9940–9941.

74 O. R. Evans, R.-G. Xiong, Z. Wang, G. K. Wong and W. Lin, *Angew. Chem.,* *Int. Ed.*, 1999, **38**, 536–538; M.-L. Tong, L.-J. Li, K. Mochizuki, H.-C. Chang, X.-M. Chen, Y. Li and S. Kitagawa, *Chem. Commun.*, 2003, 428–429.

75 R.-G. Xiong, X. Xue, H. Zhao, X.-Z. You, B. F. Abrahams and Z. Xue, *Angew. Chem., Int. Ed.*, 2002, **41**, 3800–3803; Z. P. Demko and K. B. Sharpless, *Angew. Chem., Int. Ed.*, 2002, **41**, 2110–2113; Z. P. Demko and K. B. Sharpless, *Angew. Chem., Int. Ed.*, 2002, **41**, 2113–2116; J.-P. Zhang, S.-L. Zheng, X.-C. Huang and X.-M. Chen, *Angew. Chem., Int. Ed.*, 2004, **43**, 206–209.

76 X.-X. Hu, J.-Q. Xu, P. Cheng, X.-Y. Chen, X.-B. Cui, J.-F. Song, G.-D. Yang and T.-G. Wang, *Inorg. Chem.*, 2004, **43**, 2261–2266.

77 L. Han, X.-H. Bu, Q.-C. Zhang and P.-Y. Feng, *Inorg. Chem.*, 2006, **45**, 5736–5738; J. Wang, S.-L. Zheng, S. Hu, Y.-H. Zhang and M.-L. Tong, *Inorg. Chem.*, 2007, **46**, 795–800.

78 Y. Z. Zheng, M. L. Tong and X. M. Chen, *New J. Chem.*, 2004, **28**, 1412–1415.

79 X. J. Kong, G. L. Zhuang, Y. P. Ren, L. S. Long, R. B. Huang and L. S. Zheng, *Dalton Trans.*, 2009, 1707–1709.

80 X. J. Kong, Y. P. Ren, L. S. Long, R. B. Huang, L. S. Zheng and M. Kurmoo, *CrystEngComm*, 2008, **10**, 1309–1314.

81 R. G. Lin, L. S. Long, R. B. Huang and L. S. Zheng, *Inorg. Chem. Commun.*, 2007, **10**, 1257–1261.

82 S. J. Dalgarno, J. L. Atwood and C. L. Raston, *Cryst. Growth Des.*, 2006, **6**, 174–180.

83 C. Liu, F. Luo, W. P. Liao, D. Q. Li, X. F. Wang and R. Dronskowski, *Cryst. Growth Des.*, 2007, **7**, 2282–2285.

84 S. J. Dalgarno, M. J. Hardie and C. L. Raston, *Cryst. Growth Des.*, 2004, **4**, 227–234.